

RESEARCH ARTICLE

# Heat source and sink effects on periodic mixed convection flow along the electrically conducting cone inserted in porous medium

Asifa Ilya<sup>1</sup>, Muhammad Ashraf<sup>1</sup>, Aamir Ali<sup>2</sup>, Zahir Shah<sup>3\*</sup>, Poom Kumam<sup>4,5\*</sup>, Phatiphat Thounthong<sup>6</sup>

**1** Department of Mathematics, Faculty of Science, University of Sargodha, Sargodha, Pakistan, **2** Department of Mathematics, COMSATS University Islamabad, Attock, Pakistan, **3** Department of Mathematical Sciences, University of Lakki Marwat, Lakki Marwat, Khyber Pakhtunkhwa, Pakistan, **4** Fixed Point Research Laboratory, Fixed Point Theory and Applications Research Group, Center of Excellence in Theoretical and Computational Science (TaCS-CoE), Faculty of Science, King Mongkut's University of Technology Thonburi (KMUTT), Thung Khru, Bangkok, Thailand, **5** Department of Medical Research, China Medical University Hospital, China Medical University, Taichung, Taiwan, **6** Department of Teacher Training in Electrical Engineering, Renewable Energy Research Centre, Faculty of Technical Education, King Mongkut's University of Technology North Bangkok, Bangsue, Bangkok, Thailand

\* [poom.kum@kmutt.ac.th](mailto:poom.kum@kmutt.ac.th) (PK); [zahir1987@yahoo.com](mailto:zahir1987@yahoo.com) (ZS)



**OPEN ACCESS**

**Citation:** Ilya A, Ashraf M, Ali A, Shah Z, Kumam P, Thounthong P (2021) Heat source and sink effects on periodic mixed convection flow along the electrically conducting cone inserted in porous medium. PLoS ONE 16(12): e0260845. <https://doi.org/10.1371/journal.pone.0260845>

**Editor:** Naramgari Sandeep, Central University of Karnataka, INDIA

**Received:** May 25, 2021

**Accepted:** November 18, 2021

**Published:** December 23, 2021

**Copyright:** © 2021 Ilya et al. This is an open access article distributed under the terms of the [Creative Commons Attribution License](https://creativecommons.org/licenses/by/4.0/), which permits unrestricted use, distribution, and reproduction in any medium, provided the original author and source are credited.

**Data Availability Statement:** All relevant data are within the manuscript.

**Funding:** The authors acknowledge the financial support provided by the Center of Excellence in Theoretical and Computational Science (TaCS-CoE), KMUTT. Moreover, this research project is supported by Thailand Science Research and Innovation (TSRI) Basic Research Fund: Fiscal year 2021 under project number 64A306000005. The funders had no role in study design, data collection

## Abstract

The system of partial differential equations governing the unsteady hydromagnetic boundary-layer flow along an electrically conducting cone embedded in porous medium in the presence of thermal buoyancy, magnetic field, heat source and sink effects are formulated. These equations are solved numerically by using an implicit Finite-Difference Method. The effects of the various parameters that are source/sink parameter, porous medium parameter, Prandtl number, mixed convection parameter and magnetic Prandtl number on the velocity, temperature profiles, transverse magnetic field are predicted. The effects of heat source and sink parameter on the time-mean value as well as on transient skin friction; heat transfer and current density rate are delineated especially in each plot. The extensive results reveal the existence of periodicity and show that periodicity becomes more distinctive for source and sink in the case of the electrically conducting cone. As the source and sink contrast increases, the periodic convective motion is invigorated to the amplitude and phase angle as reflect in the each plot. The dimensionless forms of the set of partial differential equations is transform into primitive form by using primitive variable formulation and then are solved numerically by using Finite Difference Scheme which has given in literature frequently. Physical interpretations of the overall flow and heat transfer along with current density are highlighted with detail in results and discussion section. The main novelty of the obtained numerical results is that first we retain numerical results for steady part and then used in unsteady part to obtain transient skin friction, rate of heat transfer and current density. The intensity of velocity profile is increased for increasing values of porosity parameter  $\Omega$ , the temperature and mass concentration intensities are reduced due heat source effects.

and analysis, decision to publish, or preparation of the manuscript.

**Competing interests:** The authors have declared that no competing interests exist.

**Abbreviations:**  $T_\infty$  (K), Ambient-temperature;  $u, v$  ( $\text{m s}^{-1}$ ), Velocity along  $xy$ -direction;  $Re_L$ , Reynolds number;  $H_x, H_y$ , Magnetic field along  $xy$ -direction (Tesla);  $Gr_L$ , Grashof number;  $\nu$  ( $\text{m}^2 \text{s}^{-1}$ ), Kinematic viscosity;  $C_p$  ( $\text{J kg}^{-1} \text{K}^{-1}$ ), The specific-heat;  $\sigma$  ( $\text{s m}^{-1}$ ), Electrical conductivity;  $\mu$  ( $\text{kg m}^{-1} \text{s}^{-1}$ ), Dynamic viscosity;  $\tau$  (Pa), Shearing stress;  $\rho$  ( $\text{kg m}^{-3}$ ), Density;  $\xi$ , Magnetic-force number;  $g$  ( $\text{m s}^{-2}$ ), Gravitational-acceleration;  $\lambda$ , Mixed-convection number;  $\beta$  ( $\text{K}^{-1}$ ), Thermal-expansion;  $\theta$ , Dimensionalized Temperature;  $v_m$  ( $\text{H m}^{-1}$ ), Magnetic-permeability;  $\gamma$ , Magnetic-Prandtl parameter;  $\alpha$  ( $\text{m}^2 \text{s}^{-1}$ ), Thermal-diffusivity;  $Pr$ , Prandtl number;  $T$  (K), Fluid Temperature.

## 1. Introduction

Several studies have been conducted on heat transport through a porous medium due to its industrial applications and numerous technical processes. Flows through porous medium are of particular interest because they are so common in nature and daily life. Water is saturated in porous materials such as sand and underground crushed rocks, which allows the fluid to move and be transported through the material under the influence of local pressure gradients. This fascination stems from the various practical applications that can be modeled or approximated, through porous medium such as packed sphere beds, high-performance building insulation, grain storage, chemical catalytic reactors, sensible heat storage beds and heat exchange between soil and atmosphere. Moreover, soil salt leaching, solar power collectors, electrochemical processes, filtering devices, insulation of nuclear reactors, regenerative heat exchangers, geothermal energy systems and many other areas. Convective heat transfer in porous medium is of much interest of research community engaged in different applied and engineering disciplines.

Kamel [1] proposed the problem of one-dimensional MHD incompressible viscous fluid flow due to heat and mass transfer through a porous medium bounded by an infinite vertical porous plate. Chamkha *et al.* [2] investigated the steady-state, hydromagnetic two dimensional forced convective boundary-layer flow of incompressible Newtonian, electrically-conducting, and heat-generating/absorbing fluid over a non-isothermal wedge with permeable surface in the existence of thermal radiation effects. He observed that as the wall mass transfer parameter is increased, both the local skin-friction coefficient and the local Nusselt number are increased. The effects of internal heat generation, suction, and injection on heat transfer in a porous medium over a stretching surface have been investigated by Elbashareshy and Bazid [3]. Cortell [4] encountered the influence of two dimensional fluid flow and heat transfer in porous medium over a stretching surface. The flow is affected by stretching the surface linearly with internal heat generation or absorption, as well as the presence of suction, blowing, and surface impermeability. He found that the Prandtl number has a tendency to lower the temperature as it rises. In the presence of a magnetic field, the issue of heat and mass transfer on a stretching sheet in a visco-elastic fluid flow through a porous medium with heat generation or absorption has been numerically investigated by Seddeek [5].

Sharma and Singh [6] predicted the problem of Variable thermal conductivity and heat source/sink impact on flow of a viscous incompressible electrically conducting fluid near a stagnation point on a non-conducting stretching layer in the presence of a uniform transverse magnetic field and variable free stream velocity. Later in the presence of a transverse magnetic field and a heat source, the effect of mass transfer on free convective flow and heat transfer of a viscous incompressible electrically conducting fluid past a vertical porous plate through a porous medium with time-dependent permeability highlighted by Das *et al.* [7]. Pal and Mondal [8]. Analyzed the effects of temperature-dependent viscosity on non-Darcy MHD mixed convective boundary layer flow and heat transfer past a porous medium in the presence of non-uniform heat source/sink. They found that the effect of non-uniform surfaces and temperature-dependent heat source/sink parameters is to produce temperature for heat source and absorb temperature for heat sink values. As a result, the cooling performance of a non-uniform heat sink is dominant. Abel *et al.* [9] conducted the analysis on the effects of laminar, two dimensional flow of an incompressible second-grade non-Newtonian liquid due to a stretching sheet through a porous medium under the influence of an external magnetic field. In the presence of a heat source or sink, the effects of thermal radiation and heat transfer over an unsteady stretching surface embedded in a porous medium have been discussed by Elbashareshy, *et al.* [10]. Osman *et al.* [11] computed the effects of thermal radiation and chemical

reactions on unsteady MHD convective flow of an incompressible fluid through a porous medium confined by an infinite vertical plate. Zheng *et al.* [12] discussed the behavior of heat transfer and boundary layer flow on time dependent permeable stretching sheet with a non-uniform heat source/sink. Later in the presence of a heat source or sink, the effects of heat transfer and thermal radiation over an unsteady stretching surface fixed in a porous medium are studied by Elbashbeshy and Emam [13].

The combined effects of a magnetic field and convective diffusion of species through a non-Darcy porous medium over a vertical non-linear stretching sheet in the existence of Ohmic dissipation and a non-uniform heat source/sink have been depicted by Pal and Mondal [14]. For transpiration cases, the effects of thermophoretic and heat source/sink parameters on MHD flow over an inclined radiate isothermal permeable surface have been explored by Noor *et al.* [15]. The combined effects of transverse magnetic field and heat source on free convective flow of viscoelastic fluid along permeable plate immersed in porous medium have been explored by Mishra *et al.* [16]. The magnetohydrodynamic convective boundary layer flow in the presence of heat generation and viscous dissipation effects past a stretching sheet inserted in porous medium carried out by Dessie and Kishan [17]. Pal and Mandal [18] discussed the effects of viscous dissipation and thermal radiation on steady two-dimensional mixed convection boundary layer flow towards a stagnation-point flow over a stretching/shrinking sheet fixed in porous medium. They found that While a sheet is stretched, the suction parameter reduces the velocity and temperature profiles, while when a sheet is shrunk, the opposite trend is observed.

Chaudhary *et al.* [19] briefly described that a boundary layer analysis is used to examine the effects of thermal radiation on the flow of an incompressible viscous electrically conducting fluid over an unsteady stretching sheet embedded in a porous medium in the presence of a heat source or drain. Sandeep and Sulochana [20] examined the influence of heat transfer of non-uniform source/sink on micropolar fluid over a stretching/shrinking sheet. The existence of a heat source/sink, MHD flow and heat transfer of a couple stress fluid over an oscillatory stretching sheet embedded in a porous medium have been illustrated by Ali *et al.* [21]. They noted that by increasing the heat source parameter, the temperature rises. In the presence of non-uniform heat source and first order chemical reaction the phenomenon of heat has been carried out to stretching sheet immersed in porous medium by Tripathy *et al.* [22]. Hayat *et al.* [23] investigated that the Internal heat generation and absorption have an effect on a nonlinear boundary layer flow of an upper-convected Maxwell (UCM) fluid over a permeable wall. The steady boundary layer magnetohydrodynamic stagnation-point flow past a stretching sheet through porous media in the presence of a heat source/sink. has been studied by Mishra *et al.* [24]. Suneetha *et al.* [25] gave an attention to the study of steady two dimensional buoyancy effects on MHD flow through a porous medium over a permeable stretching layer in the presence of suction/injection. Kumar *et al.* [26] examined the hydromagnetic three-dimensional flow of a radiating Maxwell fluid over a stretching sheet embedded in a porous medium with Soret effect and heat source/sink, first-order chemical reaction. Vijayalakshmi *et al.* [27] investigate the effects of electro magneto hydrodynamics on the fluid transportation properties of a chemically reacting Casson fluid with two different geometries. The physical behavior of the combined effect of nano particle material motion and heat generation/absorption due to the effect of different parameters involved in the prescribed flow model have been studied by Ashraf *et al.* [28]. By exerting a magnetic field exact at the surface of the magnetized cone, periodic mixed convection flow and heat transfer characteristics can be achieved by Ilyas *et al.* [29]. Unsteady, two dimensional boundary-layer fluid flow mechanism across a nonconducting horizontal circular cylinder immersed in porous medium has been carried out by Ashraf *et al.* [30]. Later, Kumar *et al.* [31–37] discussed the Newtonian and non-Newtonian

magnetohydrodynamics convective heat transfer mechanism for different characteristics of heat and fluid flow around different geometries. Dynamics of unsteady MHD flow with thermophoresis of particles and variable thermo physical properties along different shapes has been studied by Animasaun and his co-authors [38–41].

In keeping view the above literature, we interact with the phenomenon for unsteady mixed convective flow across the surface of electrically conducting cone embedded in porous medium in the presence of heat source and sink. The time dependent dimensionless equations which illustrate the hydromagnetic laminar flow along the surface of sphere are formulated. Further, we consider the motion along sphere within plume region-I with main stream velocity. By using Stokes condition we separate steady and unsteady part from the modeled partial differential equation. Later, the unsteady part is further splitted in to real and imaginary part. First we secure numerical solutions for steady part and then used in unsteady part to calculate periodic skin friction, heat transfer, and current density along the surface of the cone embedded in porous medium. We also calculate fluid velocity, magnetic field and temperature profiles, to ensure the correctness of numerical results by satisfying the prescribed boundary conditions.

### 2. Formulation and coordinate system

Consider a two-dimensional periodic mixed convection boundary-layer fluid flow along the surface of thermally and electrically conducting cone embedded in porous medium. The scheme of coordinates is shown in Fig 1. Coordinate  $x$  is measured along the surface and  $y$  is measured normally on the cone surface. The velocities  $u$  and  $v$  along the  $(x, y)$ -direction,  $H_x$  represent the component of magnetic field at the surface of cone,  $H_y$  component is taking normal to the surface of cone and external fluid velocity of the cone is  $U(x, t)$ . Moreover, magnetic field intensity proceeds exact at the surface of the cone. The form of governing dimensioned continuity, momentum, magnetic, and energy equations, as well as the boundary conditions are given as below

$$\frac{\partial u}{\partial x} + \frac{\partial v}{\partial y} = 0 \tag{1}$$

$$\epsilon^+ \left( \frac{\partial u}{\partial t} + u \frac{\partial u}{\partial x} + v \frac{\partial u}{\partial y} \right) = \epsilon^+ v \frac{\partial^2 u}{\partial y^2} + \epsilon^+ \frac{\mu}{\rho} \left( H_x \frac{\partial H_x}{\partial x} + H_y \frac{\partial H_x}{\partial y} \right) - \epsilon^{+2} \frac{\mu}{k} (u) + \epsilon^+ g\beta(T - T_\infty) \cos\left(\frac{x}{a}\right) \tag{2}$$

$$\frac{\partial H_x}{\partial x} + \frac{\partial H_y}{\partial y} = 0 \tag{3}$$

$$\frac{\partial H_x}{\partial t} + u \frac{\partial H_x}{\partial x} + v \frac{\partial H_x}{\partial y} - H_x \frac{\partial u}{\partial x} - H_y \frac{\partial u}{\partial y} = \gamma_m \frac{\partial^2 H_x}{\partial y^2} \tag{4}$$

$$\frac{\partial \theta}{\partial t} + u \frac{\partial \theta}{\partial x} + v \frac{\partial \theta}{\partial y} = \alpha \frac{\partial^2 \theta}{\partial y^2} \pm \frac{Q_o}{\rho C_p} (T - T_\infty). \tag{5}$$

The dimensioned form of boundary conditions are

$$\begin{aligned} u = v = 0, \quad H_y = 0, \quad H_x = H_0, \quad T = T_w, \quad \text{at } y = 0 \\ u \rightarrow U(\tau), \quad H_x \rightarrow 0, \quad T \rightarrow T_\infty \text{ as } y \rightarrow \infty. \end{aligned} \tag{6}$$

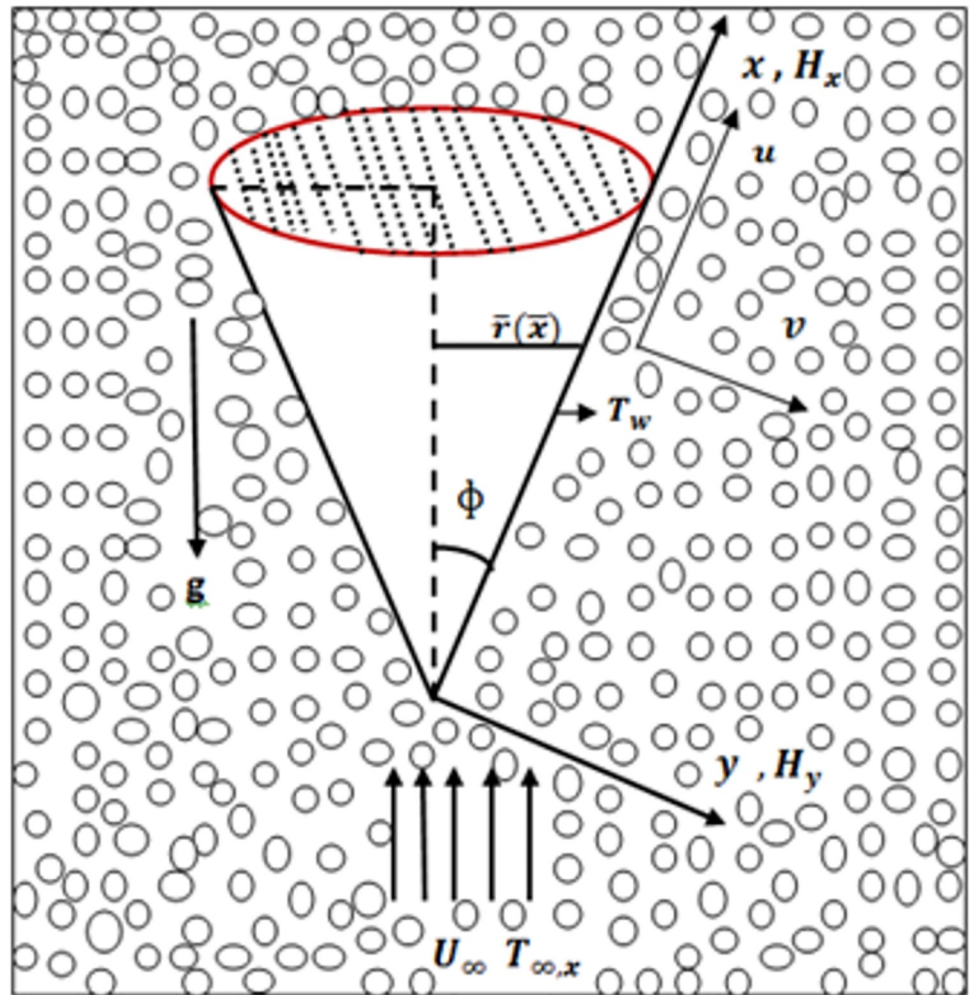


Fig 1. Electrically conducting cone and coordinate system.

<https://doi.org/10.1371/journal.pone.0260845.g001>

The following are the dimensionless system of coupled nonlinear partial differential equations:

$$\frac{\partial \bar{u}}{\partial \bar{x}} + \frac{\partial \bar{v}}{\partial \bar{y}} = 0 \tag{7}$$

$$\frac{\partial \bar{u}}{\partial \tau} + \bar{u} \frac{\partial \bar{u}}{\partial \bar{x}} + \bar{v} \frac{\partial \bar{u}}{\partial \bar{y}} = \frac{\partial^2 \bar{u}}{\partial \bar{y}^2} + \zeta \left( \bar{h}_x \frac{\partial \bar{h}_x}{\partial \bar{y}} + \bar{h}_y \frac{\partial \bar{h}_x}{\partial \bar{y}} \right) - \Omega(\bar{u}) + \lambda \bar{\theta} \tag{8}$$

$$\frac{\partial \bar{h}_x}{\partial \bar{x}} + \frac{\partial \bar{h}_y}{\partial \bar{y}} = 0 \tag{9}$$

$$\frac{\partial \bar{h}_x}{\partial \tau} + \bar{u} \frac{\partial \bar{h}_x}{\partial \bar{x}} + \bar{v} \frac{\partial \bar{h}_x}{\partial \bar{y}} - \bar{h}_x \frac{\partial \bar{u}}{\partial \bar{x}} - \bar{h}_y \frac{\partial \bar{u}}{\partial \bar{y}} = \frac{1}{\gamma} \frac{\partial^2 \bar{h}_x}{\partial \bar{y}^2} \tag{10}$$

$$\frac{\partial \bar{\theta}}{\partial \tau} + \bar{u} \frac{\partial \bar{\theta}}{\partial \bar{x}} + \bar{v} \frac{\partial \bar{\theta}}{\partial \bar{y}} = \frac{1}{Pr} \frac{\partial^2 \bar{\theta}}{\partial \bar{y}^2} \pm \delta \theta. \tag{11}$$

The dimensionless boundary conditions are:

$$\begin{aligned} \bar{u} = \bar{v} = 0, \quad \bar{h}_y = 0, \quad \bar{h}_x = 1, \quad \bar{\theta} = 1, \quad \text{at } \bar{y} = 0 \\ \bar{u} \rightarrow \bar{U}(\tau), \quad \bar{\theta} \rightarrow 0, \quad \bar{h}_x \rightarrow 0, \quad \text{as } \bar{y} \rightarrow \infty. \end{aligned} \tag{12}$$

The third and fourth term on right hand side of Eq (8) which are  $\Omega$  and  $\lambda$ , represents porosity number and mixed convection dimensionless number,  $\gamma$  is Prandtl magnetic number, Prandtl parameter is  $Pr$ ,  $H_o$  is the exact strength of the magnetic field at the surface and  $\delta$  represents the heat generation absorption parameter.

$$\begin{aligned} \zeta = \frac{\mu H_0^2}{\rho U_\infty^2}, \quad \alpha = \frac{\kappa}{\rho C_p}, \quad \lambda = \frac{G_{rL}}{Re_L^2}, \quad Re_L = \frac{U_\infty L}{\nu}, \quad Dal = \frac{k}{\epsilon^+ L^2}, \quad Pr = \frac{\nu}{\alpha}, \quad G_{rL} \\ = \frac{g \beta \Delta T L^3}{\nu^2} \cos \alpha, \quad \gamma = \frac{\nu}{\nu_m}, \quad \Omega = \frac{1}{D_{al} Re_L}, \quad \delta = \frac{Q_o L}{\rho C_p U_\infty}. \end{aligned} \tag{13}$$

The stream velocity under  $|\epsilon| \ll 1$ , where  $\epsilon$  presents a small magnitude periodic component and the frequency parameter  $\omega$  is takes the term  $U(\tau) = 1 + \epsilon e^{i\omega\tau}$ . The velocity of the fluid, magnetic field and temperature components  $u, v, h_x, h_y$  and  $\theta$  are defined as the sum of steady and unsteady equations.

$$\begin{aligned} \bar{u} = u_s + \epsilon u_t e^{i\omega\tau}, \quad \bar{v} = v_s + \epsilon v_t e^{i\omega\tau}, \quad \bar{h}_x = h_{xs} + \epsilon h_{xt} e^{i\omega\tau} \\ \bar{h}_y = h_{ys} + \epsilon h_{yt} e^{i\omega\tau}, \quad \bar{\theta} = \theta_s + \epsilon \theta_t e^{i\omega\tau}. \end{aligned} \tag{14}$$

By following orders  $O(\epsilon^0)$  and  $O(\epsilon e^{i\omega\tau})$ , using these orders from Eqs (7-11) using proposed boundary-conditions (12), we can separately replace dimensionless steady and unsteady equations by using Eq (14) in the form of:

**For steady components:**

$$\frac{\partial u_s}{\partial x} + \frac{\partial v_s}{\partial y} = 0 \tag{15}$$

$$u_s \frac{\partial u_s}{\partial x} + v_s \frac{\partial u_s}{\partial y} = \frac{\partial^2 u_s}{\partial y^2} + \zeta \left( h_{xs} \frac{\partial h_{xs}}{\partial x} + h_{ys} \frac{\partial h_{ys}}{\partial y} \right) - \Omega u_s + \lambda \theta_s \tag{16}$$

$$\frac{\partial h_{xs}}{\partial x} + \frac{\partial h_{ys}}{\partial y} = 0 \tag{17}$$

$$u_s \frac{\partial h_{xs}}{\partial x} + v_s \frac{\partial h_{xs}}{\partial y} - h_{xs} \frac{\partial u_s}{\partial x} - h_{ys} \frac{\partial u_s}{\partial y} = \frac{1}{\gamma} \frac{\partial^2 h_s}{\partial y^2} \tag{18}$$

$$u_s \frac{\partial \theta_s}{\partial x} + v_s \frac{\partial \theta_s}{\partial y} = \frac{1}{Pr} \frac{\partial^2 \theta_s}{\partial y^2} \pm \delta \theta_s \tag{19}$$

with appropriate boundary conditions:

$$\begin{aligned} u_s = v_s = 0, \quad h_{ys} = 0, \quad h_{xs} = 1, \quad \theta_s = 1 \quad \text{at } y = 0 \\ u_s \rightarrow 1, \quad \theta_s \rightarrow 0, \quad h_{xs} \rightarrow 0 \quad \text{as } y \rightarrow \infty. \end{aligned} \tag{20}$$

By taking into consideration the Stokes second problem or sometimes referred to as oscillating boundary layer given in Eq (21) to split the unsteady variables into imaginary part and real part. Thus the separate form of the imaginary and real equations can be computed by using the equation Eq (21) given below.

$$\begin{aligned} u_t = u_1 + iu_2, \quad v_t = v_1 + iv_2, \quad \theta_t = \theta_1 + i\theta_2, \\ h_{xt} = h_{x1} + ih_{x2}, \quad h_{yt} = h_{y1} + ih_{y2}. \end{aligned} \tag{21}$$

For real components:

$$\frac{\partial u_1}{\partial x} + \frac{\partial v_1}{\partial y} = 0 \tag{22}$$

$$-\omega u_2 + u_s \frac{\partial u_1}{\partial x} + u_1 \frac{\partial u_s}{\partial x} + v_s \frac{\partial u_1}{\partial y} + v_1 \frac{\partial u_s}{\partial y} = \frac{\partial^2 u_1}{\partial y^2} + \zeta \left( h_{xs} \frac{\partial h_{x1}}{\partial x} + h_{x1} \frac{\partial h_{xs}}{\partial x} + h_{ys} \frac{\partial h_{x1}}{\partial y} + h_{y1} \frac{\partial h_{ys}}{\partial y} \right) - \Omega u_1 + \lambda \theta_1 \tag{23}$$

$$\frac{\partial h_{x1}}{\partial x} + \frac{\partial h_{y1}}{\partial y} = 0 \tag{24}$$

$$-\omega h_{x2} + u_s \frac{\partial h_{x1}}{\partial x} + u_1 \frac{\partial h_{xs}}{\partial x} + v_s \frac{\partial h_{x1}}{\partial y} + v_1 \frac{\partial h_{xs}}{\partial y} - h_{xs} \frac{\partial u_1}{\partial x} - h_{x1} \frac{\partial u_s}{\partial x} - h_{ys} \frac{\partial u_1}{\partial y} - h_{y1} \frac{\partial u_s}{\partial y} = \frac{1}{\gamma} \frac{\partial^2 h_{x1}}{\partial y^2} \tag{25}$$

$$-\omega \theta_2 + u_s \frac{\partial \theta_1}{\partial x} + u_1 \frac{\partial \theta_s}{\partial x} + v_s \frac{\partial \theta_1}{\partial y} + v_1 \frac{\partial \theta_s}{\partial y} = \frac{1}{P_r} \frac{\partial^2 \theta_1}{\partial y^2} \pm \delta \theta_1 \tag{26}$$

along with boundary conditions:

$$\begin{aligned} u_1 = v_1 = 0, \quad h_{y1} = 0, \quad h_{x1} = 0, \quad \theta_1 = 0 \quad \text{at } y = 0 \\ u_1 \rightarrow 1, \quad \theta_1 \rightarrow 0, \quad h_{x1} \rightarrow 0 \quad \text{as } y \rightarrow \infty. \end{aligned} \tag{27}$$

For imaginary components:

$$\frac{\partial u_2}{\partial x} + \frac{\partial v_2}{\partial y} = 0 \tag{28}$$

$$\omega u_1 + u_s \frac{\partial u_2}{\partial x} + u_2 \frac{\partial u_s}{\partial x} + v_s \frac{\partial u_2}{\partial y} + v_2 \frac{\partial u_s}{\partial y} = \frac{\partial^2 u_2}{\partial y^2} + \zeta \left( h_{xs} \frac{\partial h_{x2}}{\partial x} + h_{x2} \frac{\partial h_{xs}}{\partial x} + h_{ys} \frac{\partial h_{x2}}{\partial y} + h_{y2} \frac{\partial h_{ys}}{\partial y} \right) - \Omega u_2 + \lambda \theta_2 \tag{29}$$

$$\frac{\partial h_{x2}}{\partial x} + \frac{\partial h_{y2}}{\partial y} = 0 \tag{30}$$

$$\omega h_{x1} + u_s \frac{\partial h_{x2}}{\partial x} + u_2 \frac{\partial h_{xs}}{\partial x} + v_s \frac{\partial h_{x2}}{\partial y} + v_2 \frac{\partial h_{xs}}{\partial y} - h_{xs} \frac{\partial u_2}{\partial x} - h_{x2} \frac{\partial u_s}{\partial x} - h_{ys} \frac{\partial u_2}{\partial y} - h_{y2} \frac{\partial u_s}{\partial y} = \frac{1}{\gamma} \frac{\partial^2 h_{x2}}{\partial y^2} \tag{31}$$

$$\omega \theta_1 + u_s \frac{\partial \theta_2}{\partial x} + u_2 \frac{\partial \theta_s}{\partial x} + v_s \frac{\partial \theta_2}{\partial y} + v_2 \frac{\partial \theta_s}{\partial y} = \frac{1}{P_r} \frac{\partial^2 \theta_2}{\partial y^2} \pm \delta \theta_2 \tag{32}$$

along with boundary conditions:

$$\begin{aligned} u_2 = v_2 = 0, \quad h_{y2} = 0, \quad h_{x2} = 0, \quad \theta_2 = 0, \quad \text{at } y = 0 \\ u_2 \rightarrow 0, \quad \theta_2 \rightarrow 0, \quad h_{x2} \rightarrow 0, \quad \text{as } y \rightarrow \infty. \end{aligned} \tag{33}$$

### 3. Solution methodology

The system of equations give in (15)–(19) and (22)–(32) along with boundary conditions have been transform into primitive form by following [28–30] for integration. Later, we use Finite Difference procedure which is based on the well-documented repute in literature. Spatial differencing schemes of second-order accuracy were used for the equation terms. A central differencing was selected for the diffusion terms (Ilyas et al. [29]) was adopted to discretize the nonlinear convective terms. The general form of the system of obtained algebraic equations can be expressed as.

$$A\Gamma_{(i-1,j)} + B\Gamma_{(i,j)} + C\Gamma_{(i+1,j)} = D$$

Here,  $\Gamma$  represent the field variable  $u, v, \theta, h_x$  and  $h_y$  respectively, where  $A, B, C$  and  $D$  are coefficient matrices for above mentioned unknown variables. Later, the coefficient matrices are solved by using Gaussian elimination technique. Convergence of the solutions was declared at each step by following.

$$\max|\Gamma^{n+1} - \Gamma^n| \leq 10^{-5}$$

Where  $n$  represent the  $n$ th iteration.

In actual computations, first the steady-state solutions are obtained and then are used for the solution of unsteady system of equations. Later, the obtained steady and unsteady solutions are used to calculate periodic skin friction  $\tau_s$ , heat transfer  $\tau_t$  and current density  $\tau_m$  along the electrically conducting cone, where  $A_s, A_t$  and  $A_m$  are amplitudes while,  $\alpha_s, \alpha_t$  and  $\alpha_m$  are phase angles (see [30]).

$$\tau_w = \left(\frac{\partial U}{\partial Y}\right)_{y=0} + \varepsilon|A_s|\text{Cos}(\omega t + \alpha_s), \quad q_w = \left(\frac{\partial \theta}{\partial Y}\right)_{y=0} + \varepsilon|A_t|\text{Cos}(\omega t + \alpha_t), \tag{34}$$

$$j_w = \left(\frac{\partial \varphi}{\partial Y}\right)_{y=0} + \varepsilon|A_m|\text{Cos}(\omega t + \alpha_m),$$

where

$$A_s = (u_1^2 + u_2^2)^{\frac{1}{2}}, \quad A_t = (\theta_1^2 + \theta_2^2)^{\frac{1}{2}}, \quad A_m = (\varphi_{x1}^2 + \varphi_{x2}^2)^{\frac{1}{2}},$$

$$\alpha_s = \tan^{-1}\left(\frac{u_2}{u_1}\right), \quad \alpha_t = \tan^{-1}\left(\frac{\theta_2}{\theta_1}\right), \quad \alpha_m = \tan^{-1}\left(\frac{\varphi_{x2}}{\varphi_{x1}}\right).$$

### 4. Results and discussions for steadiness and periodical behavior

A model Stokes boundary layer problem in which buoyancy plays a significant role has been formulated for flow along a thermally and electrically conducting cone embedded in a porous medium. The situation of Stokes boundary layer depends on the effects of different parameters involved in the fluid flow model. The results also show that depending upon the orientation of the surface, buoyancy forces acting on the heated fluid near the surface of the cone alter the flow such that the processes is accelerated or delayed. The solutions for the various values of the parameters involved in the flow model show that there is a strong coupling between the



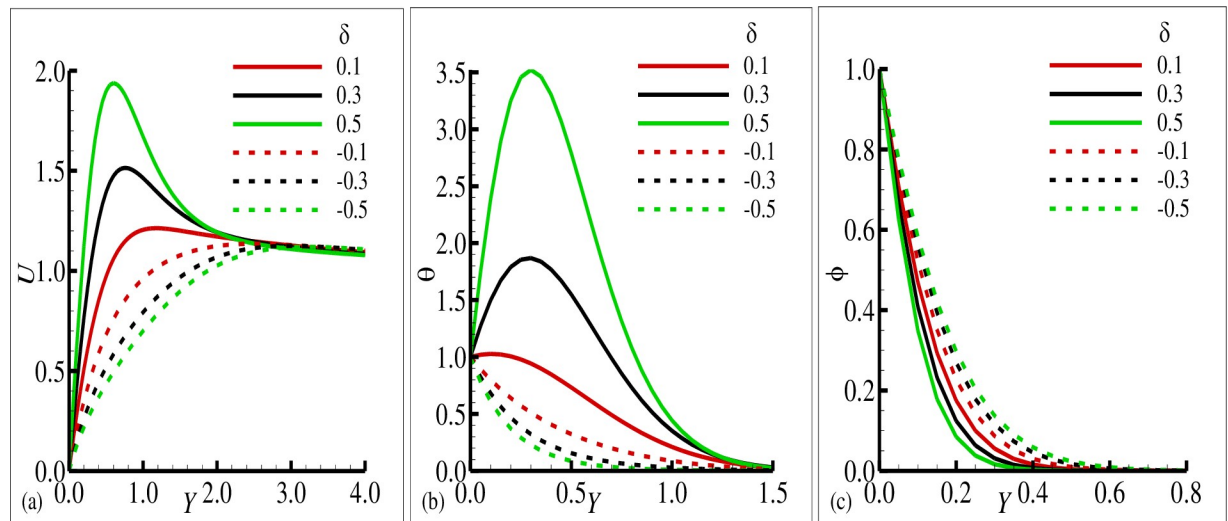


**Fig 2.** The graphical results for (a) velocity field  $u$ , (b) temperature field  $\theta$ , and (c) magnetic field  $\phi$  with various values of  $\delta = 0.1, 0.5, 1.0$  for heat source and  $\delta = -0.1, -0.5, -1.0$  for sink, where others are  $\gamma = 0.5$ ,  $Pr = 7.0$ ,  $\xi = 0.2$ ,  $\lambda = 0.1$  and  $\Omega = 0.05$ .

<https://doi.org/10.1371/journal.pone.0260845.g002>

fluid flow and heat transfer within the boundary layer. In this study, we are particularly concerned with the computational analysis of the characteristics of heat and fluid flow mechanism along the coordinate system depicted in Fig 1. With this understanding the detail discussion of the obtained results is given in the below paragraphs.

Fig 2(A)–2(C) reported typical velocity, temperature, and transverse magnetic field profiles in the boundary layer along the surface of cone for various values of the source sink parameter  $\pm\delta$  (+ sign indicates source and (–) sign indicates the sink), respectively. In these figures, it is shown that the velocity component  $U$  and the temperature variable ( $\theta$ ) is increased as the values of the source parameter ( $+\delta$ ) is increased and these components are reduced for the sink parameter ( $-\delta$ ). It is also shown the transverse component of magnetic field ( $\phi$ ) is reduced for the source parameter ( $+\delta$ ) but on the other hand it is slightly increased for the increasing values of sink parameter ( $-\delta$ ). It is pertinent to point out that the solid lines in each plot is seen the effects of source parameter while the dashed lines highlights the effects of sink parameter. The phenomena in Fig 3(A)–3(C) illustrate the effects of the various values of the Prandtl number  $Pr$  on the velocity component  $U$ , temperature variable ( $\theta$ ) and transverse magnetic field variable ( $\phi$ ) in the simultaneous presence of source and sink parameter ( $\delta = \pm 0.6$ ). It is concluded that the increase in Prandtl number  $Pr$  is reduced the velocity component  $U$  and the temperature variable ( $\theta$ ) in both cases that is source and sink while the transverse component of magnetic ( $\phi$ ) is increased in both source and sink regions. The effects of the mixed convection parameter  $\lambda$  on the velocity component, temperature variable and transverse magnetic field are reflected in Fig 4(A)–4(C), for source sink parameter  $\delta = \pm 0.7$  respectively. In these plots, it can be seen for increasing values of mixed convection parameter  $\lambda$  the velocity component  $U$  is increased and variable temperature and transverse magnetic field are reduced with the same trend simultaneously both for source and sink parameter ( $\delta = \pm 0.7$ ). Fig 5(A)–5(C) depict the influence of the porous medium parameter  $\Omega$  on the velocity component  $U$ , temperature variable ( $\theta$ ) and transverse magnetic field ( $\phi$ ) for  $\delta = \pm 0.9$  respectively. It is observed that imposition of porous medium parameter increases the velocity component and decreases the temperature variable ( $\theta$ ) for source parameter and the transverse magnetic field is reduced for sink parameter ( $-\delta$ ) and no changes are observed for the case of source parameter ( $+\delta$ ).

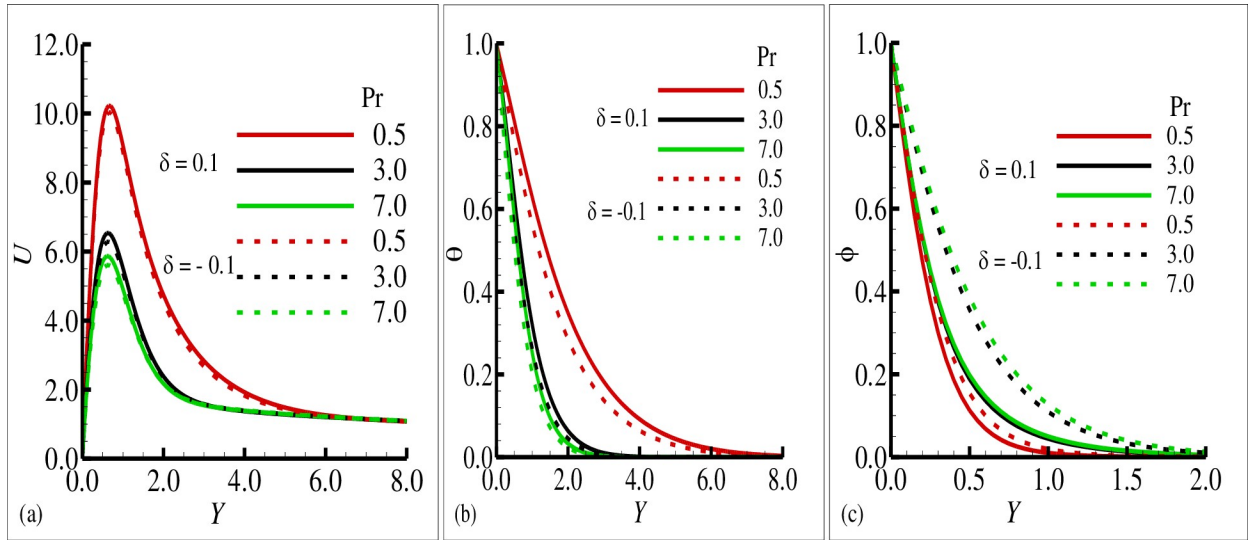


**Fig 3.** The graphical results for (a) velocity field  $u$ , (b) temperature field  $\theta$ , and (c) magnetic field  $\phi$  with choice values of  $Pr = 0.5, 3.0, 7.0$  for heat source  $\delta = 0.6$  and sink  $\delta = -0.6$ , where others are  $\gamma = 0.4, \lambda = 0.2, \xi = 0.8$ , and  $\Omega = 0.5$ .

<https://doi.org/10.1371/journal.pone.0260845.g003>

The influence of the source and sink parameter  $\pm\delta$  on the periodical skin friction, heat transfer and current density is presented in Fig 6(A)–6(C), respectively. This is due to the reason that because of the increase in sink parameter the heated surface is transfer its energy to the fluid which is at lower temperature than the surface temperature. The second reason is that due to an increase in source parameter the constant heat parameter  $Q_0$  is increase and kinetic motion of the fluid particle is decreased. In these plots it is very clear that amplitude of periodic skin friction is increased for increasing values of source parameter  $\delta$  and is reduced in the sink ranges. In the case of periodical heat transfer this trend is reversed, the amplitude of periodic heat transfer is increased in the sink range and reduced in the source range. It is important to point out that the periodical current density is uniform in both rages. The behavior of

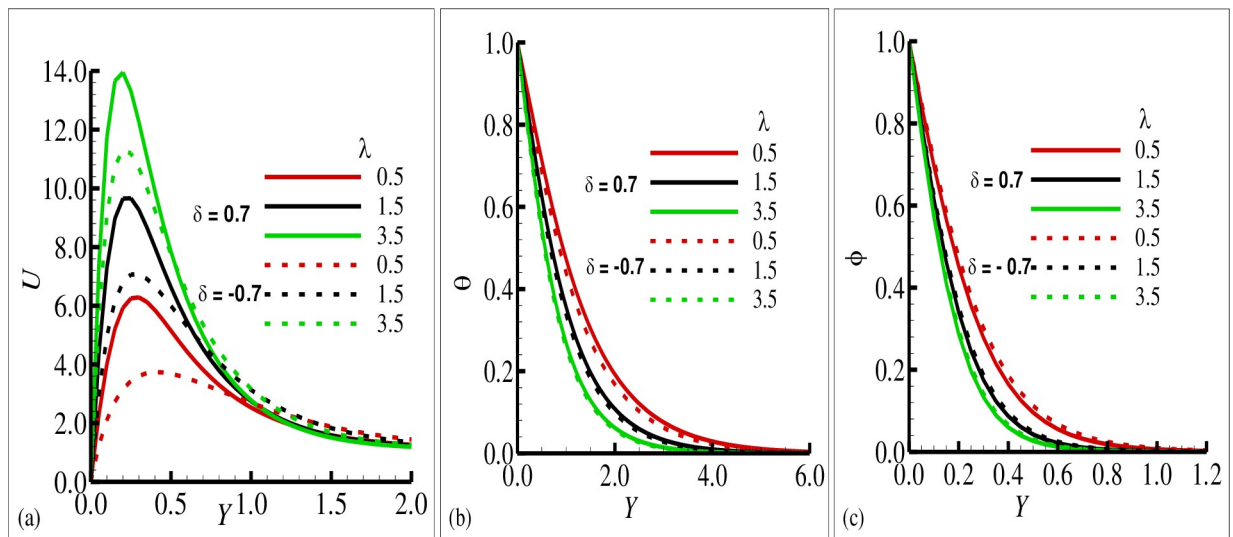


**Fig 4.** The graphical results for (a) velocity field  $u$ , (b) temperature field  $\theta$ , and (c) magnetic field  $\phi$  with the choice values of  $\lambda = 0.5, 1.5, 3.5$  for heat source  $\delta = 0.7$  and sink  $\delta = -0.7$ , where others are  $\gamma = 0.3, \Omega = 0.06, \xi = 0.7$  and  $Pr = 7.0$ .

<https://doi.org/10.1371/journal.pone.0260845.g004>

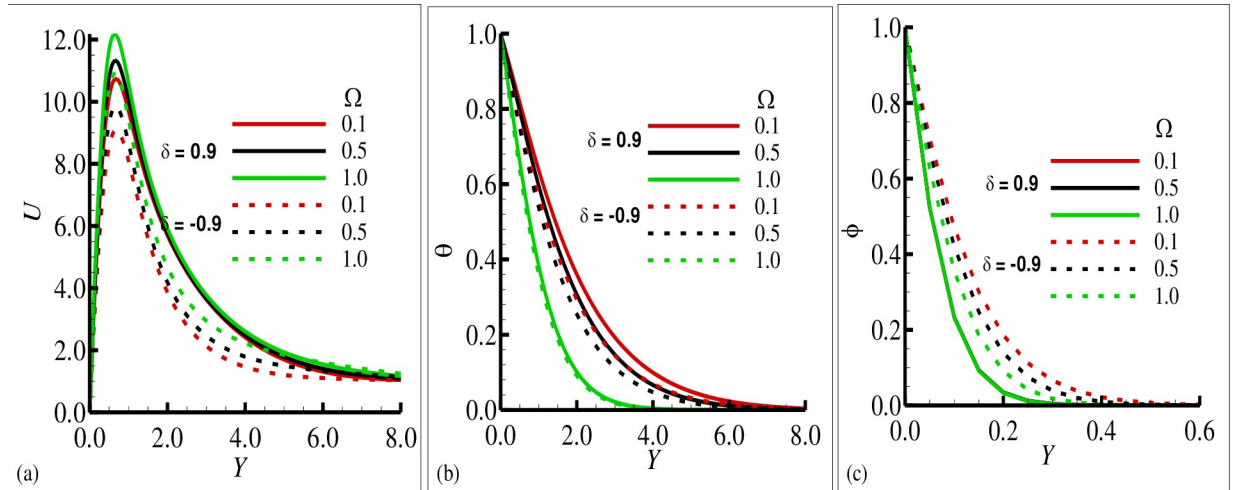


**Fig 5.** The graphical results for (a) velocity field  $u$ , (b) temperature field  $\theta$ , and (c) magnetic field  $\phi$  with the choice values of  $\Omega = 0.1, 0.5, 1.0$  for heat source  $\delta = 0.9$  and sink  $\delta = -0.9$ , where others are  $\gamma = 0.4, Pr = 7.0, \xi = 0.5$  and  $\lambda = 0.1$ .

<https://doi.org/10.1371/journal.pone.0260845.g005>

periodical skin friction, heat transfer and current density is highlighted in Fig 7(A)–7(C) for different values of magnetic Prandtl number  $\gamma$  in source and sink range respectively. From these figures it is depicted that the amplitude of periodic skin friction is increased for source range and is reduced for sink range, but the periodic heat transfer is increased in sink region and is uniformly distributed in each range. In Fig 7(C) it is noted that the periodic current density is increased with the increasing values of  $\gamma$  and particularly uniformly distributed in source and sink range. The physical reasoning depicted in Fig 7(A)–7(C) is due to the fact that for increasing values of magnetic Prandtl number  $\gamma$  the magnetic diffusion rate is dominant over viscous diffusion rate. In Fig 8(A)–8(C), the increase of porous medium parameter  $\Omega$  clearly leads to significant decrease in both the periodic skin friction and heat transfer. However, there is no change is noted in the case of periodic current density. It was expected because for increasing values of the porous medium parameter  $\Omega$  the total amount of void space accessible from the surface or phase boundary is increased. From the inspection of Fig 9(A)–9(C), it reveals that for increasing values of mixed convection parameter  $\lambda$  the amount of periodic skin friction is increased in the heat source range while the reverse trend is noted in the case of

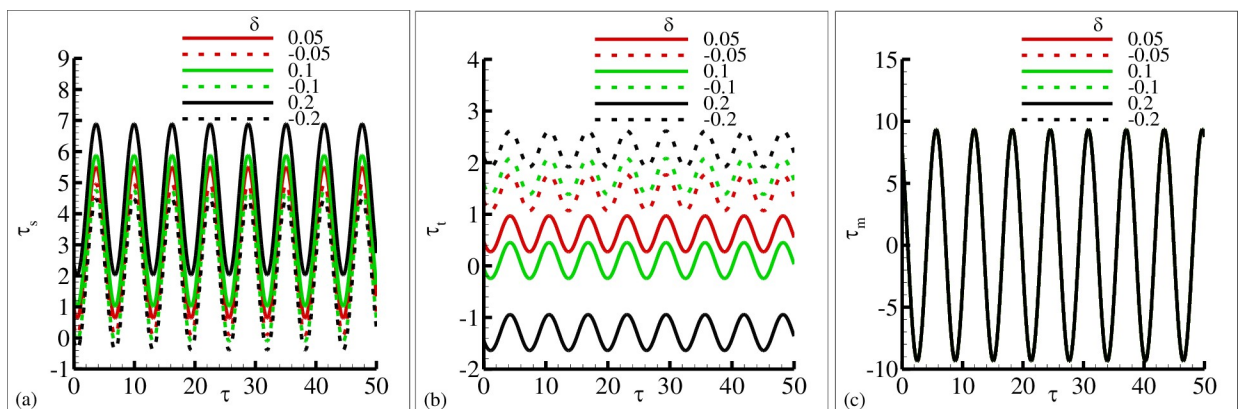


**Fig 6.** The graphical results of (a)  $\tau_w$  (b)  $q_w$  and (c)  $j_w$  for various values of heat source  $\delta = 0.05, 0.1, 0.2$  and heat sink  $\delta = -0.05, -0.1, -0.2$ , where other parameters  $\gamma = 1.6, \xi = 0.6, Pr = 7.0, \Omega = 1.5$  and  $\lambda = 7.5$ .

<https://doi.org/10.1371/journal.pone.0260845.g006>

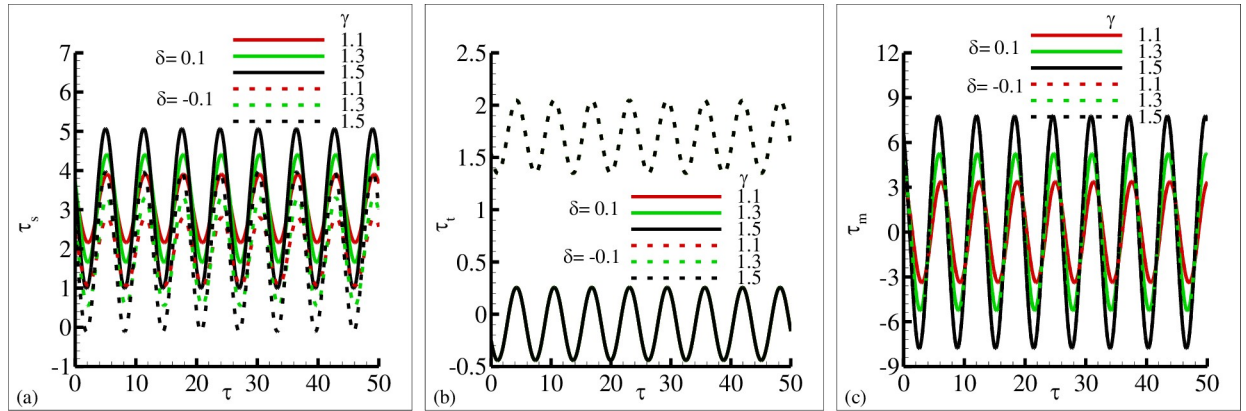


**Fig 7.** The graphical results of (a)  $\tau_w$  (b)  $q_w$  and (c)  $j_w$  for various values of  $\gamma = 1.1, 1.3, 1.5$  for heat source  $\delta = 0.1$  and sink  $\delta = -0.1$ , where other parameters  $\lambda = 6.2, \xi = 0.2, Pr = 7.0$ , and  $\Omega = 1.7$ .

<https://doi.org/10.1371/journal.pone.0260845.g007>

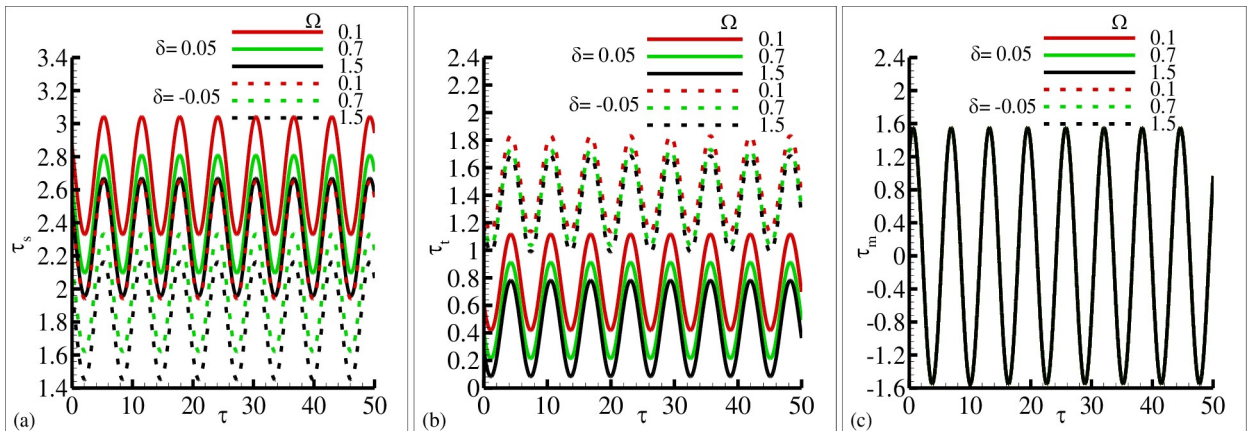


**Fig 8.** The graphical results of (a)  $\tau_w$  (b)  $q_w$  and (c)  $j_w$  for various values of  $\Omega = 0.1, 0.7, 1.5$  for heat source  $\delta = 0.05$  and sink  $\delta = -0.05$ , where other parameters  $\gamma = 0.8, \xi = 0.3, Pr = 7.0$ , and  $\lambda = 5.1$ .

<https://doi.org/10.1371/journal.pone.0260845.g008>

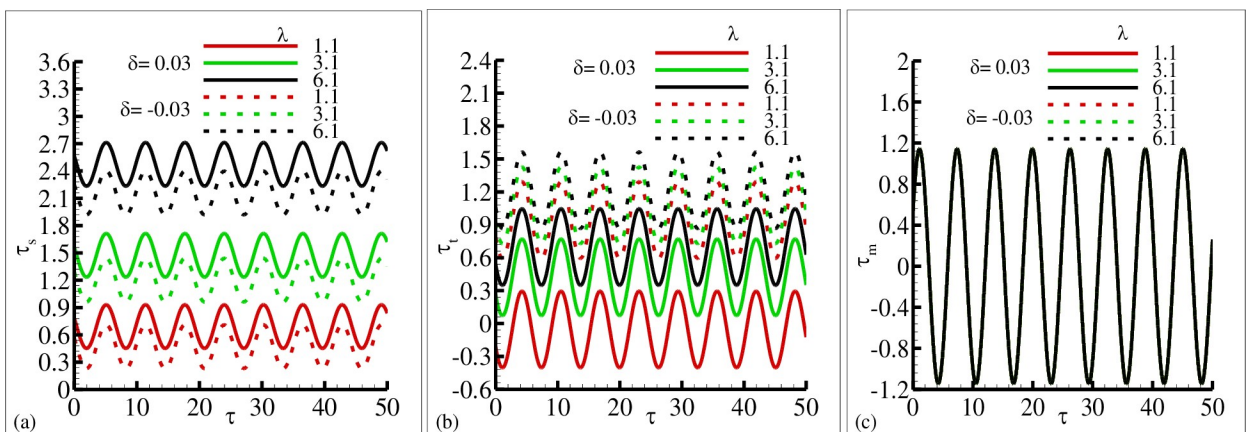


**Fig 9.** The graphical results of (a)  $\tau_w$  (b)  $q_w$  and (c)  $j_w$  for various values of  $\lambda = 1.1, 3.1, 6.1$  for heat source  $\delta = 0.03$  and sink  $\delta = -0.03$ , where other parameters  $\Omega = 1.7, \xi = 0.8, Pr = 7.0$ , and  $\gamma = 0.7$ .

<https://doi.org/10.1371/journal.pone.0260845.g009>

periodic heat transfer, mean to say the heat sink is significantly dominated. It is important to define that the mixed convection parameter is the ratio of the buoyancy force to flow shear force. The mechanism predicted in Fig 9(A)–9(C) is due to the reason for the increasing values of mixed convection parameter  $\lambda$  that buoyancy force is dominant over flow shear force.

## 5. Conclusions

In this paper, the occurrence of periodic/oscillatory convection flow along the surface of electrically conducting cone has been investigated numerically. For this purpose, comprehensive numerical solutions have been obtained to delineate the effect of different parameters involved in the flow model on velocity, temperature field and transverse magnetic field along with periodic skin friction, heat transfer and current density. Characteristics of the transient periodic/oscillatory convection appear largely in skin friction and heat transfer and in some cases of periodic current density. The main objective of this study is to investigate the impact of heat source and sink parameter periodic/oscillatory skin friction, heat transfer and current density.

In this study we conclude that intensity of heat and fluid flow is effective in the case of heat source and the heat sink effects are dominated by heat source. Moreover, heat source and sink are not prominent in the case of current density. It is noted that due to domination of the buoyancy force which acts like a pressure gradient the velocity profile, periodic skin friction is increased on the other hand temperature, transverse magnetic field, periodic heat transfer and current density are reduced. Due to the increase of porous medium parameter the void space accessible from the surface is increased thus a very significant reduction in periodic skin friction and heat transfer is noted. It is claimed that because of the prevailing attitude of the magnetic diffusion over viscous diffusion the velocity profile, temperature distribution, transverse magnetic field, periodic skin friction, periodic heat transfer, periodic current density are appreciably affected.

## Author Contributions

**Conceptualization:** Zahir Shah.

**Formal analysis:** Zahir Shah.

**Funding acquisition:** Poom Kumam, Phatiphat Thounthong.

**Investigation:** Asifa Ilya, Aamir Ali, Poom Kumam, Phatiphat Thounthong.

**Methodology:** Zahir Shah.

**Project administration:** Muhammad Ashraf, Poom Kumam, Phatiphat Thounthong.

**Resources:** Aamir Ali, Poom Kumam, Phatiphat Thounthong.

**Software:** Aamir Ali.

**Supervision:** Poom Kumam.

**Validation:** Aamir Ali, Poom Kumam, Phatiphat Thounthong.

**Visualization:** Zahir Shah.

**Writing – review & editing:** Aamir Ali, Zahir Shah.

## References

1. Kamel MH. Unsteady MHD convection through porous medium with combined heat and mass transfer with heat source/sink. *Energy Conversion and Management*. 2001 Mar 1; 42(4):393–405.

2. Chamkha AJ, Mujtaba M, Quadri A, Issa C. Thermal radiation effects on MHD forced convection flow adjacent to a non-isothermal wedge in the presence of a heat source or sink. *Heat and Mass Transfer*. 2003 Apr; 39(4):305–12.
3. Elbashbeshy EM, Bazid MA. Heat transfer in a porous medium over a stretching surface with internal heat generation and suction or injection. *Applied mathematics and computation*. 2004 Nov 15; 158(3):799–807.
4. Cortell R. Flow and heat transfer of a fluid through a porous medium over a stretching surface with internal heat generation/absorption and suction/blowing. *Fluid Dynamics Research*. 2005 Oct; 37(4):231.
5. Seddeek MA. Heat and mass transfer on a stretching sheet with a magnetic field in a visco-elastic fluid flow through a porous medium with heat source or sink. *Computational Materials Science*. 2007 Feb 1; 38(4):781–7.
6. Sharma PR, Singh G. Effects of variable thermal conductivity and heat source/sink on MHD flow near a stagnation point on a linearly stretching sheet.
7. Das SS, Satapathy A, Das JK, Panda JP. Mass transfer effects on MHD flow and heat transfer past a vertical porous plate through a porous medium under oscillatory suction and heat source. *International journal of heat and mass transfer*. 2009 Dec 1; 52(25–26):5962–9.
8. Pal D, Mondal H. Effect of variable viscosity on MHD non-Darcy mixed convective heat transfer over a stretching sheet embedded in a porous medium with non-uniform heat source/sink. *Communications in Nonlinear Science and Numerical Simulation*. 2010 Jun 1; 15(6):1553–64.
9. Abel MS, Mahesha N, Malipatil SB. Heat transfer due to MHD slip flow of a second-grade liquid over a stretching sheet through a porous medium with nonuniform heat source/sink. *Chemical Engineering Communications*. 2010 Oct 29; 198(2):191–213.
10. Elbashbeshy EM, Yassmin DM, Dalia AA. Heat transfer over an unsteady porous stretching surface embedded in a porous medium with variable heat flux in the presence of heat source or sink. *African Journal of Mathematics and Computer Science Research*. 2010 May 31; 3(5):68–73.
11. Osman AN, Abo-Dahab SM, Mohamed RA. Analytical solution of thermal radiation and chemical reaction effects on unsteady MHD convection through porous media with heat source/sink. *Mathematical Problems in Engineering*. 2011 Jan 1; 2011.
12. Zheng L, Wang L, Zhang X. Analytic solutions of unsteady boundary flow and heat transfer on a permeable stretching sheet with non-uniform heat source/sink. *Communications in Nonlinear Science and Numerical Simulation*. 2011 Feb 1; 16(2):731–40.
13. Elbashbeshy E, Emam TG. Effects of thermal radiation and heat transfer over an unsteady stretching surface embedded in a porous medium in the presence of heat source or sink. *Thermal science*. 2011; 15(2):477–85.
14. Pal D, Mondal H. Hydromagnetic convective diffusion of species in Darcy–Forchheimer porous medium with non-uniform heat source/sink and variable viscosity. *International Communications in Heat and Mass Transfer*. 2012 Aug 1; 39(7):913–7.
15. Noor NF, Abbasbandy S, Hashim I. Heat and mass transfer of thermophoretic MHD flow over an inclined radiate isothermal permeable surface in the presence of heat source/sink. *International Journal of Heat and Mass Transfer*. 2012 Mar 1; 55(7–8):2122–8.
16. Mishra SR, Dash GC, Acharya M. Mass and heat transfer effect on MHD flow of a visco-elastic fluid through porous medium with oscillatory suction and heat source. *International Journal of Heat and Mass Transfer*. 2013 Feb 1; 57(2):433–8.
17. Dessie H, Kishan N. MHD effects on heat transfer over stretching sheet embedded in porous medium with variable viscosity, viscous dissipation and heat source/sink. *Ain shams engineering journal*. 2014 Sep 1; 5(3):967–77.
18. Pal D, Mandal G. Mixed convection–radiation on stagnation-point flow of nanofluids over a stretching/shrinking sheet in a porous medium with heat generation and viscous dissipation. *Journal of Petroleum Science and Engineering*. 2015 Feb 1; 126:16–25.
19. Chaudhary S, Choudhary MK, Sharma R. Effects of thermal radiation on hydromagnetic flow over an unsteady stretching sheet embedded in a porous medium in the presence of heat source or sink. *Mechanica*. 2015 Aug; 50(8):1977–87.
20. Sandeep N, Sulochana C. Dual solutions for unsteady mixed convection flow of MHD micropolar fluid over a stretching/shrinking sheet with non-uniform heat source/sink. *Engineering Science and Technology, an International Journal*. 2015 Dec 1; 18(4):738–45.
21. Ali N, Khan SU, Sajid M, Abbas Z. MHD flow and heat transfer of couple stress fluid over an oscillatory stretching sheet with heat source/sink in porous medium. *Alexandria Engineering Journal*. 2016 Jun 1; 55(2):915–24.

22. Tripathy RS, Dash GC, Mishra SR, Hoque MM. Numerical analysis of hydromagnetic micropolar fluid along a stretching sheet embedded in porous medium with non-uniform heat source and chemical reaction. *Engineering science and technology, an international journal*. 2016 Sep 1; 19(3):1573–81.
23. Hayat T, Awais M, Imtiaz A. Heat source/sink in a magneto-hydrodynamic non-Newtonian fluid flow in a porous medium: dual solutions. *Plos one*. 2016 Sep 6; 11(9):e0162205. <https://doi.org/10.1371/journal.pone.0162205> PMID: 27598314
24. Mishra SR, Nayak B, Sharma RP. MHD stagnation-point flow past over a stretching sheet in the presence of non-Darcy porous medium and heat source/sink. In *Defect and Diffusion Forum 2017* (Vol. 374, pp. 92–105). Trans Tech Publications Ltd.
25. Suneetha K, Ibrahim SM, Reddy GR. Radiation and heat source effects on MHD flow over a permeable stretching sheet through porous stratum with chemical reaction. *Multidiscipline Modeling in Materials and Structures*. 2018 Dec 6.
26. Kumar SG, Varma S, Prasad PD, Raju CS, Makinde OD, Sharma R. MHD reacting and radiating 3-D flow of Maxwell fluid past a stretching sheet with heat source/sink and Soret effects in a porous medium. In *Defect and Diffusion Forum 2018* (Vol. 387, pp. 145–156). Trans Tech Publications Ltd.
27. Vijayalakshmi P, Gunakala SR, Animasaun IL, Sivaraj R. Chemical Reaction and Nonuniform Heat Source/Sink Effects on Casson Fluid Flow over a Vertical Cone and Flat Plate. In *Applied Mathematics and Scientific Computing: International Conference on Advances in Mathematical Sciences, Vellore, India, December 2017-Volume II 2019 Feb 1* (p. 117). Springer.
28. Ashraf M, Abbas A, Zia S, Chu YM, Khan I, Nisar KS. Computational Analysis of the Effect of Nano Particle Material Motion on Mixed Convection Flow in the Presence of Heat Generation and Absorption. *CMC-COMPUTERS MATERIALS & CONTINUA*. 2020 Jan 1; 65(2):1809–23.
29. Ilyas A, Ashraf M. Periodic mixed convection flow along the surface of a thermally and electrically conducting cone. *Thermal Science*. 2020; 24(Suppl. 1):225–35.
30. Ashraf M, Ullah Z, Zia S, Alharbi SO, Baleanu D, Khan I. Analysis of the Physical Behavior of the Periodic Mixed-Convection Flow around a Nonconducting Horizontal Circular Cylinder Embedded in a Porous Medium. *Journal of Mathematics*. 2021 Jan 25; 2021.
31. Kumar KA, Sugunamma V, Sandeep N. Effect of thermal radiation on MHD Casson fluid flow over an exponentially stretching curved sheet. *Journal of Thermal Analysis and Calorimetry*. 2020 Jun; 140(5):2377–85.
32. Anantha KK, Buruju RR, Sandeep N, Vangala S. Effect of Joule heating on MHD non-Newtonian fluid flow past an exponentially stretching curved surface. *Heat Transfer*.
33. Kumar KA, Sugunamma V, Sandeep N. Thermophoresis and Brownian Motion Effects on MHD Micropolar Nanofluid Flow Past a Stretching Surface With Non-uniform Heat Source/Sink. *Computational Thermal Sciences: An International Journal*. 2020; 12(1).
34. Kumar KA, Sugunamma V, Sandeep N. Influence of viscous dissipation on MHD flow of micropolar fluid over a slendering stretching surface with modified heat flux model. *Journal of Thermal Analysis and Calorimetry*. 2020 Mar; 139(6):3661–74.
35. Tilili I, Mustafa MT, Kumar KA, Sandeep N. Effect of asymmetrical heat rise/fall on the film flow of magnetohydrodynamic hybrid ferrofluid. *Scientific reports*. 2020 Apr 21; 10(1):1–1. <https://doi.org/10.1038/s41598-019-56847-4> PMID: 31913322
36. Kumar KA, Sugunamma V, Sandeep N, Mustafa MT. Simultaneous solutions for first order and second order slips on micropolar fluid flow across a convective surface in the presence of Lorentz force and variable heat source/sink. *Scientific reports*. 2019 Oct 11; 9(1):1–4. <https://doi.org/10.1038/s41598-018-37186-2> PMID: 30626917
37. Kumar A, Sugunamma V, Sandeep N, JV RR. Impact of Brownian motion and thermophoresis on bio-convective flow of nanoliquids past a variable thickness surface with slip effects. *Multidiscipline Modeling in Materials and Structures*. 2019 Jan 7.
38. Animasaun IL. Dynamics of unsteady MHD convective flow with thermophoresis of particles and variable thermo-physical properties past a vertical surface moving through binary mixture. *Open Journal of Fluid Dynamics*. 2015 Jun; 5(02):106–120.
39. Shah NA, Animasaun IL, Ibraheem RO, Babatunde HA, Sandeep N, Pop I. Scrutinization of the effects of Grashof number on the flow of different fluids driven by convection over various surfaces. *Journal of Molecular liquids*. 2018 Jan; 249: 980–990.
40. Shah NA, Animasaun IL, Chung JD, Wakif A, Alao FI, Raju CS. K. Significance of nanoparticle's radius, heat flux due to concentration gradient, and mass flux due to temperature gradient: the case of water conveying copper nanoparticles. *Scientific Reports*. 2021 Jan; 11(1):1 <https://doi.org/10.1038/s41598-020-79139-8> PMID: 33414495

41. Sowmya G, Gireesha BJ, Animesaun I L, Shah NA. Significance of buoyancy and Lorentz forces on water-conveying iron (III) oxide and silver nanoparticles in a rectangular cavity mounted with two heated fins: heat transfer analysis. *Journal of Thermal Analysis and Calorimetry*. 2021 Feb; 1–16.